Synthesis of lignin/ graphene oxide/polyurethane composite and itsapplication as an adsorbent for polynuclear aromatic hydrocarbon removal from wastewater

M. G. Taha [a], S. M. Elhamamsy [a], , Y. Moustafa [b] M. Elshafie [b]

[a] Agricultural Biochemistry Department, Faculty of Agriculture, Al-Azhar University, Nasr City, Cairo, Egypt.

[b] Analysis and Evaluation Department, Egyptian Petroleum Research Institute, 11727 Nasr City, Cairo, Egypt.

Abstract: Lignin/graphene-oxide/polyurethane composite was synthesized in order to evaluate its performance as an adsorbent for polynuclear aromatic hydrocarbons PAHs. The sequence of this process are lignin extraction and graphene-oxide preparation as a precursor for lignin/graphene-oxide/polyurethane composites synthesis. Characterization of this composite was carried out using elemental analysis, FTIR, X-ray, gel permeation chromatography GPC, and transmission electron microscopy TEM. An experimental design according to the Taguchi orthogonal array approach using Minitab software was carried out to enables the effect of factors on the response to be ascertained and identifies the optimal experimental conditions with the least variability. The efficiency of this composite towards polyaromatic removal was investigated using high performance liquid chromatography HPLC and compared to that obtained for the precursor materials. i.e., lignin and graphene oxide.

1.Introduction

Lignin, the second most naturally abundant biomass, which makes up 15% to 35% of the cell walls of terrestrial plants [1], [2]. Lignin is an excellent raw material for preparing chemicals because of its rich sources and low price. Lignin has abundant functional groups, such as hydroxyl, benzyl, methoxyl, ether, carboxyl, etc., resulting in its amphiphilic nature. Hydroxyl is the most important functional group for lignin modifications including alkylation, esterification, phenolation, hydoxypropylation [3]. Extracted lignin from the paper industry is employed as concrete additives, stabilizing agents or dispersants and surfactants[4]. Lignin could potentially solve the problem of the rapidly depleting resources if it was successfully translated into a renewable resource or valorized to higher value materials[1].

Recently, Lignin has several applications in high-value utilization to Synthesize Ag Nanoparticles[5]; lignin graft copolymers, lignin-thermosetting polymer systems and lignin-elastomer systems[6]. Polyurethane containing lignin, ligin-based carbon fibers [7], lignosulfonates can be used as surfactants or dispersants in various applications such as chelating agents, water reducers of cement, dye dispersants, etc. [8], [9].

The objective of this work is to evaluate and develop a sustainable cost-effective material derived from pulping industries waste specifically lignin. Furthermore, the utilization of this prepared material in petroleum effluent treatment for removing polynuclear aromatic hydrocarbon from discharged wastewater. The methodology for this study is to extract lignin from black liquor, prepare graphene-oxide, and Functionalize both lignin and graphene oxide with polyurethane link L-GO-PU.

Experimental

1.   Lignin extraction

Kraft lignin was separated from this concentrated pulping liquor using a solidification method [10] by concentrated H_2SO_4 (70%) followed by a neutralization stage. 1-liter black liquor was firstly

diluted with 3-liter DI-H$_2$O to reduce viscosity and pH to 11-12. Subsequent, 500 mL of concentrated H$_2$SO$_4$ was mildly added with a rate of 1.5 ml/min under continuous stirring at which the dissolved Na-lignin convert to non-dissolved brown floated KL "H-lignin" solids (pH≈ 3 - 3.5). The obtained sulfonated KL product was washed with hot DI-H$_2$O till neutralization (pH≈ 6 – 6.5), after which it was dried at 323K till constant weight (yield ≈ 340± 50 g per 1L liquor).

2.   Graphene oxide preparation

Graphite 3g were mixed with 18 potassium permanganate [11] with a ratio of 1:6 respectively. Then 400 ml of the acid mixture of sulfuric acid and nitric acid with the ratio of 9:1 respectively added to the solid mixture and the color became dark green. The mixture was stirred for 12 hours at 50 °C. The mixture let to cool then 400 ml of deionized water added while stirring. Finally, 6 ml of H$_2$O$_2$ added the mix then the solution turned to a brown-yellowish color. The reaction product decanted and washed at least three times with deionized water then washed 5 times with centrifugation and dried in an oven at 60 °C.

3.   Synthesis of L-GO-PU

The reaction performed between two components A and B with a ratio of 1:1.1 weight percent. A is a polyol mixture of 0.4 lignin and 0.1 graphene oxide and 0.5 castor oil mixed with a mechanical stirrer. Component B is the methylene diphenyl diisocyanate (MDI) heated in n-pentane at 60 °C is mixed with component A for 10 minutes by mechanical stirrer and the temperature kept at 60 °C.

The final product washed by n-hexane to remove unreacted materials.

4.   Characterization

Elemental analysis was performed in an automatic analyzer, Elementar, vario Macro CHNS Element Analyzer. The oxygen content was calculated by subtraction of the sum of carbon, hydrogen, sulfur, and nitrogen from 100 %. The FTIR analysis carried out in the Egyptian Petroleum Research Institute, Central laboratories, using PerkinElmer spectrometer model, spectrum one. The FTIR spectra of extracted lignin, the prepared graphene-oxide,

and the synthesized lignin/graphene-oxide/polyurethane are represented in Figures (1). The phase structures were determined by X-ray powder diffraction (XRD, Xpert PRO, PAN analytical, Netherlands) at 1.54056 Å using Cu Kα radiation 2θ angle from 5 to 80°. X-ray graphs for lignin, graphene oxide and Lignin/Graphene-oxide/Polyurethane are shown in Figures (2). The extracted lignin characterized by using Gel Permeation Chromatography (GPC) to determine the number average molecular weights (Mn), weight average molecular weights (Mw), and polydispersity index (Mw/Mn). Gel permeation chromatography (GPC) was performed at 30°C using GPC-Water 2410, coupled with a refractive index detector. A column styragel HR THF 7.8 × 300 mm was used in separation, and equipped with a Waters 515 HPLC pump. THF was used as an eluent at a flowrate of 1 ml/min. Aliquots (1 ml) of lignin sample was diluted with an appropriate amount of THF and shaken vigorously, then passed through a filter and injected into the GPC for analysis. Transmission electron microscopy (TEM) images were recorded on a JEOL JEM-2, 100 electron microscope at 200 kV accelerating voltage. Samples for TEM were prepared by placing a drop of lignin, graphene oxide, or lignin/graphene oxide/ polyurethane dispersion on a carbon-coated copper grid and let dry at room temperature.

5.   Experimental design

The orthogonal array is the key feature of Taguchi experimental design which asses the effects of factors on the response mean and variation. Three effects of three factors were studied, contact time, dose and pH of the solution, using L18 design shown in table (1). Anthracene removal were calculated using Eq. (1)

$$Removal \% = \left(\frac{c_0 - c_e}{c_0} \right) \times 100 \quad (1)$$

where C$_0$ and C$_e$ were the initial and equilibrium concentrations of Anthracene (mg/L), respectively. Signal to noise ratio is calculated according to the "larger-is-better" theorem as represented in equation (2).

$$\frac{S}{n} = \frac{-10 \log \sum_{i=1}^{n} \frac{1}{y_i^2}}{n} \quad (2)$$

n was the number of repetitions under the same experimental conditions, and y_i represented the measurement results. The bottles contained 10 ml of 1 mg anthracene solution. The adsorbent was removed from water samples by centrifugation then the concentration of the residual anthracene measured in HPLC.

6. High performance liquid chromatography HPLC:

The amount of anthracene was measured in water without pretreatment using high-performance liquid chromatography HPLC Agilent Infinity 1200 fitted with a UV photodiode array PDA detector. The HPLC system was fitted with a 4.6 by 250-mm reverse-phase C18 column, using acetonitrile: water 70:30 as the mobile phase at a flow rate of 1 ml min^{-1}. Sample solutions (30 μL) were injected into the HPLC system using an autosampler Suppelco C18 column as a stationary phase. The excitation wavelength of PAHs was 254 nm for anthracene.

Table (1): Taguchi orthogonal array applied in this study

Time (hr)	pH	Dose (g/L)
1	6	1
1	7	5
1	8	10
2	6	1
2	7	5
2	8	10
4	6	5
4	7	10
4	8	1
6	6	10
6	7	1
6	8	5
12	6	5
12	7	10
12	8	1
24	6	10
24	7	1
24	8	5

7. Adsorption kinetics study:

The affinity between the adsorbent and the adsorbate was the main factor controlling the adsorption [12]. In order to investigate the sorption process mechanism and the potential rate controlling adsorption of anthracene onto lignin, graphene oxide, and L-GO-PU, kinetic models have been used. Pseudo-first order and pseudo-second-order kinetic models were

tested for obtained data to elucidate the adsorption mechanism. The best fit model was selected based on the linear regression correlation coefficient R^2 values.

Lagergren's first-order rate equation has been most widely used for the adsorption of adsorbate from an aqueous solution. It is represented in equation (3),

$$\log(q_e - q_t) = \log q_e - \frac{K}{2.303}t \quad (3)$$

where q_e is the equilibrium adsorption capacity (mg/g), q_t is the mass of metal ions adsorbed at time t (mg/g), K is the pseudo-first-order rate constant (min^{-1}).

The pseudo-second-order rate equation is represented in equation (4),

$$\frac{t}{q_t} = \frac{1}{k_2 q_e^2} + \frac{t}{q_e} \quad (4)$$

Where, K_2 is the pseudo second order rate constant.

The possibility of intra-particle diffusion resistance which could affect the adsorption is explored by using the intra-particle diffusion model given in the equation (5)

$$q_t = k_i t^{1/2} + C \quad (5)$$

Where, k_i is the intra-particle diffusion rate constant, and C is the intercept.

Results and Discussion

1. Elemental analysis

The elemental analysis data of lignin, graphene oxide and L-GO-PU are listed in table (2). The Elemental analyses of materials under study reflect their chemical composition. Elemental analysis of extracted lignin showed that the lignin comprises 51.22% carbon, 19.33% hydrogen, 22.93% oxygen, 1.4% nitrogen and sulfur content of 5.12 %. The low nitrogen content in extracted lignin is possibly due to protein contamination in the lignin during pulping process. For the preparation of graphene oxide from graphite the results confirmed the oxidation of graphite as the graphene oxide comprises 40.97% carbon, 46.51% oxygen, 10.9% hydrogen, and sulfur content 1.39%. Furthermore, the prepared lignin graphene oxide polyurethane composite contains a higher percentage of carbon of 73.91% and lower oxygen content with 6.89%,

this may be due to the addition of castor oil in the polyurethane molecules.

1. FTIR

The FT-IR analysis was carried out to identify the characteristic peaks of lignin (L), graphene oxide (GO), and Lignin/Graphene-oxide/polyurethane are shown in Figure. (1).

Table (2) elemental analysis of lignin, graphene oxide and L-GO-PU composite

Material	C%	H%	N%	S%	O%
Lignin	51.2	19.3	1.4	5.1	22.9
Graphene Oxide	41.0	10.9	<1%	1.3	46.5
L-GO-PU Composite	73.9	7.2	10.6	1.4	6.9

Lignin spectrum shows bands at 2956 and 2847 cm^{-1} were assigned for the asymmetric and symmetric stretching vibrations of methylene groups, respectively, and the broadband around 3400 cm^{-1} are characteristic for O–H stretching. The absorption band at 1700 cm^{-1} is due to the carbonyl stretching. The peak at 1040 cm^{-1} is allocated to aromatic C-H in plane deformation. The corresponding vibrational frequencies for the stretching mode are around 3400 cm^{-1}, 1090cm^{-1} and 1700cm^{-1}, for hydroxyl (OH), epoxy (C-O-C) and ketone (C=O) groups respectively.

A typical FTIR spectrum of graphene-oxide is reported in the obtained vibration frequencies: hydroxyl broadband around 3450 cm^{-1}, carbonyls 1700 – 1850 cm^{-1}, carboxyl 1650 – 1700 cm^{-1}, and ethers/epoxides 1000–1280 cm^{-1}

The FTIR spectrum of the L/GO/PU confirmed the presence of urethane linkages, as represented by the prominent peaks at 2920 and 2853 cm^{-1} that are attributed to C–H stretching of CH$_3$ and CH$_2$ and –NH asymmetric stretching in the vibration region (3200–3500 cm^{-1} 1). The peaks at 1721, 1606, and 1223 cm^{-1} 1 are associated with C=O stretching in the amide, urea and ether groups, respectively, and the peak at 1526 cm1 is attributed to the amide II band.

2. X-ray Diffraction analysis

Figure (2) compiles the XRD pattern for lignin, Graphene oxide/ Lignin. graphene oxide polyurethane composite. Lignin exhibits two broad, weak diffraction peaks (2θ = 10°-30°,35°-50°) that are attributable to amorphous cross-linked phenylpropane-based polymers oriented in a random fashion [13]. X-ray diffraction (XRD) pattern of graphene oxide shows only a broad peak around 11° This peak is associated with the interlayer distance ~1 nm due to the presence of functional groups onto GO [14]. The XRD pattern for the synthesized composite shows a broad peak related to the amorphous structure or a weak crystallinity which is obverse with the crystal nature of lignin-based polyurethane [15].

3. Gel Permeation Chromatography GPC

Molecular weight of the extracted lignin was determined by GPC, the lignin was eluted from the column and detected at 28.2 min. The number average weight (Mn) of the lignin was 1464 while weight average weight (Mw) was 2096, with a polydispersity index of 1.435. The weight of the lignin was determined by comparing with the weight of the polystyrene standards used for calibration.

4. Transmission electron microscopy TEM

TEM images of lignin, graphene oxide and lignin graphene oxide polyurethane are shown in Fig. 3. The morphology of the synthesized polymer is the same as the precursor
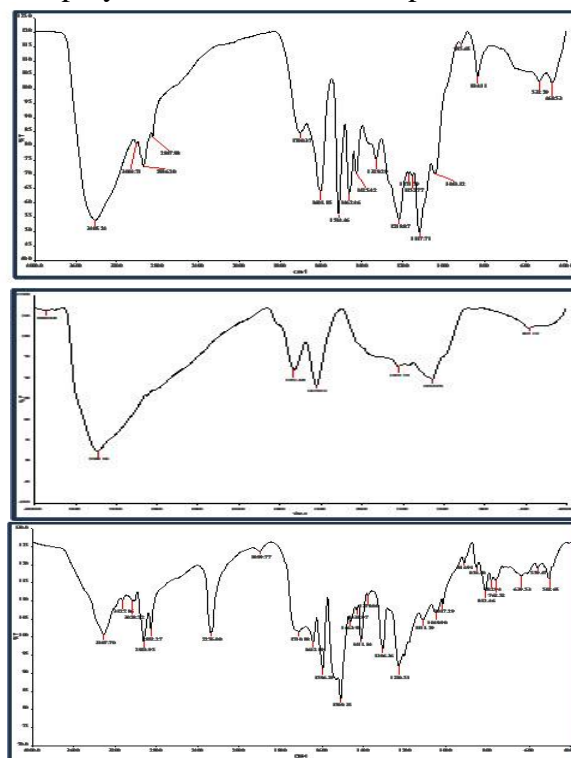

Fig (1): FT-IR spectrum of the lignin (A), graphene oxide (B) and

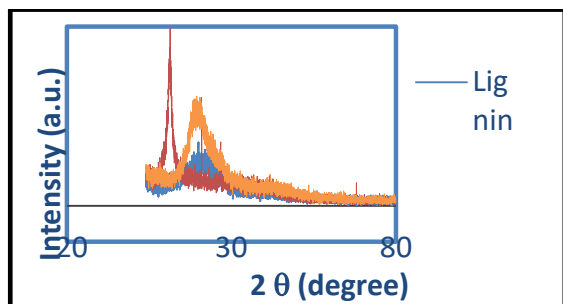**synthesized lignin/graphene-oxide/polyurethane composite (C).**

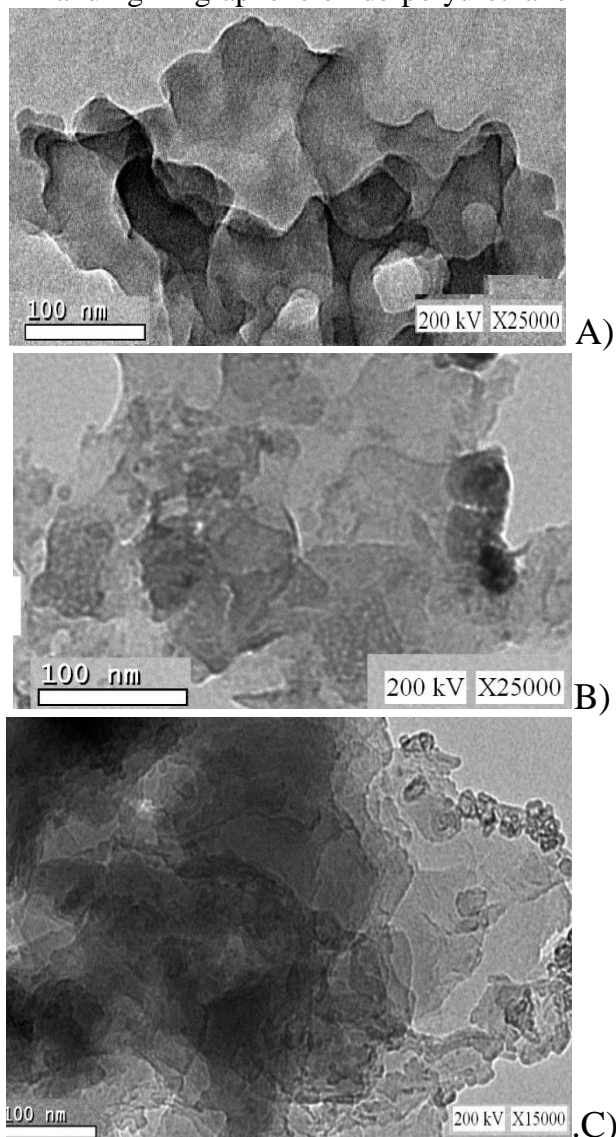**Fig (2):** XRD for lignin, graphene oxide GO, and lignin-graphene oxide-polyurethane

Fig (3): TEM images of; (A) lignin, (B) graphene oxide, and (C) lignin-graphene oxide-polyurethane.

Amorphous structure of lignin and lignin polyurethane is observed from the morphology represented in figure (3 A ,B and C) and possess an irregular surface and deep grooves with diameters exceed 100 nanometers which may be capable to captivate polynuclear aromatic hydrocarbons. The image of graphene oxide presented in Figure (3 B) shows the transparent and single sheet-like structure that prove the production of graphene oxide sheets by chemical exfoliation.

5.   Batch adsorption results:

Results of anthracene removal percentage obtained due to use of lignin, GO, and L-GO-PU are presented in Table (3). In general, the initial observation of obtained results from performed experiments showed that extracted lignin has a low to moderate efficiency that it achieves 89% anthracene removal after 24 hours using 10 g/L adsorbent. However, L-GO-PU composite attained almost the same efficiency after 1 hour using 5g/L adsorbent.

In comparison between GO and L-GO-PU composite, it is observed that 10 g/L of GO achieves 98% anthracene removal in two hours. However, the same dosage (10 g/L) of L-GO-PU composite can remove the same percentage 98% after one hours.

Thus, L/GO/PU composite exhibits higher efficiency for anthracene removal than unmodified lignin owing to its increased hydrophobicity rather than its raw materials components

Table (3): The removal percent of anthracene

Time (hr)	pH	Dose (g/L)	Lignin	GO	L-GO PU
1	6	1	29.34	63.15	68.06
1	7	5	69.82	84.65	87.19
1	8	10	78.96	95.88	98.03
2	6	1	48.01	81.44	75.43
2	7	5	62.50	88.43	88.27
2	8	10	74.20	98.17	98.73
4	6	5	78.34	98.10	91.45
4	7	10	82.19	98.89	98.98
4	8	1	74.13	89.21	83.92
6	6	10	87.22	99.08	99.01
6	7	1	75.39	98.28	98.09
6	8	5	80.20	98.19	98.68
12	6	5	81.26	98.28	98.68
12	7	10	88.21	99.13	99.08
12	8	1	76.64	98.37	98.49
24	6	10	89.19	99.17	99.02
24	7	1	77.10	98.45	98.63
24	8	5	83.15	98.33	98.94

Signal to noise ratio obtained using Minitab is listed in Table (4), and also related S/N ratio for each level of every individual controllable

factor using L-GO-PU was drawn in Fig. 6, which elucidated the core of Taguchi method. Fig. 6 showed that the largest S/N variation occurred with contact time, followed by adsorbent dose, and change in pH. In other words, the most significant controllable factor was contact time while the least significant one was change in pH. Another method for ranking is the value of delta calculated using Minitab and listed in Table (4). A larger delta value implied a more significant factor and should be utilized first. The range in descending order was contact time > Dose > pH. This trend was further checked by analysis of variance (ANOVA) statistical approach using Minitab. The results of ANOVA showed the same order of influence on the anthracene removal as illustrated in Table (5) by sum of square (SS) of individual controllable factor. Namely, the highest contribution was contact time, followed

by adsorbent dose, and change in solution pH. Hence from data obtained, the optimum condition for operating the process of removing anthracene from water using lignin is, contact time 12 hr, pH 7, and dose 10 g/L; moreover, the optimum condition for using L-GO-PU is contact time 6 h, pH 7, and dose 10 g/L Data represented in table (6) shows the significance of different factors under study in the form of percentage of contribution (p-value). Adsorbent dose possessed a significant effect on

anthracene removal process with p-value 0.007 and 0.017 for lignin and L-GO-PU respectively. Furthermore, contact time retained effect on adsorption process while p-values were 0.017 and 0.036 for lignin and L-GO-PU respectively. On the other hand, solution pH has no significant effect on anthracene adsorption.

Table (4): Response Table for Signal to Noise Ratios

Level	Lignin			L-GO-PU			GO		
	Time (hr)	pH	Dose (g/L)	Time (h)	pH	Dose (g/L)	Time (h)	pH	Dose (g/L)
1	31.01	27.71	30.32	19.38	13.11	15.659	18.78	10.13	11.852
2	31.34	27.09	27.28	17.09	8.56	11.251	10.65	5.36	5.670
3	26.66	26.80	23.99	14.31	6.43	1.192	4.60	3.64	1.614
4	25.30			2.648			1.48		
5	24.75			1.756			1.41		
6	24.14			1.022			1.35		
Delta	7.21	0.92	6.33	18.354	6.682	14.468	17.424	6.488	10.238
Rank	**1**	**3**	**2**	**1**	**3**	**2**	**1**	**3**	**2**

Adsorption kinetics

The pseudo-first-order model considers the rate of occupation of adsorption sites is directly proportional to the number of unoccupied sites. A plot of log $(q_e - q_t)$ against t should give a linear relationship for the applicability of the pseudo-first-order kinetic. Figure (5) represents the Pseudo-First-order sorption kinetics of anthracene on to lignin, graphene oxide
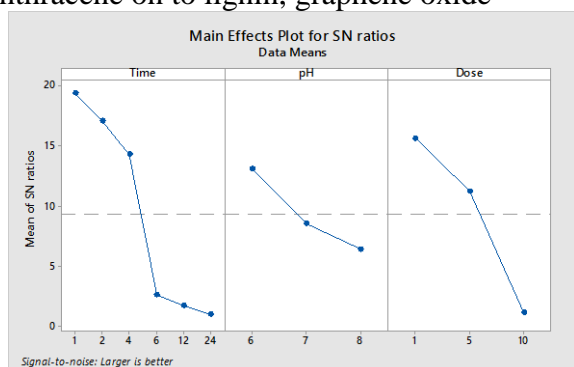
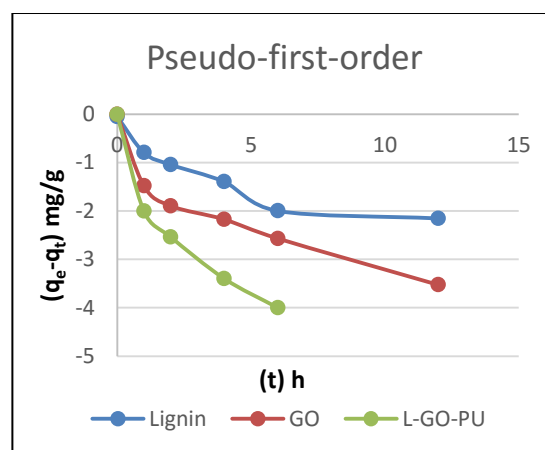**Fig (4):** Signal to noise ratio plot for L-GO-P U

Fig (5): The pseudo-first-order kinetic sorption for lignin, GO, L-GO-PU

The Pseudo-second-order model considers that the rate of adsorption is based on the square of the number of vacant sites on the adsorbent. A plot of t/q_t versus t should give a linear relationship for the applicability of the pseudo-second-order kinetic model shown in figure (6)
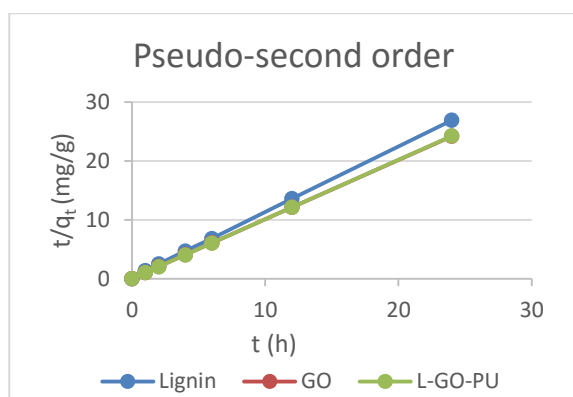
Fig (6): pseudo-second-order sorption kinetics for lignin, GO, and L-GO-PU.

The correlation coefficients shown in table (6) are closer to unity for pseudo-second-order kinetics than for pseudo-first-order kinetics. This suggests that the adsorption system can be better represented by the pseudo-second-order model [16]. For materials used in this study according to R^2 calculated were 0.9999 for lignin and 1 fo GO and L-GO-PU which confirms the applicability of the pseudo-second order equation. This suggests that the overall rate of the anthracene adsorption process appears to be controlled by the chemisorption

Table (5): Analysis of Variance for Means

Adsorbent	Source	DF	Seq SS	Adj SS	Adj MS	F	P
Lignin	**Time (h)**	5	1747.0	1747.0	349.41	5.54	0.017
	pH	2	266.9	266.9	133.46	2.12	0.183
	Dose (g/L)	2	1212.2	1212.2	606.08	9.62	0.007
	Residual Error	8	504.2	504.2	63.02		
	Total	17	3730.3				
GO	**Source**	DF	Seq SS	Adj SS	Adj MS	F	P
	Time (h)	5	747.1	747.1	149.43	4.00	0.041
	pH	2	135.6	135.6	67.79	1.81	0.224
	Dose (g/L)	2	319.0	319.0	159.48	4.26	0.055
	Residual Error	8	299.2	299.2	37.39		
	Total	17	1500.8				
L-GO-PU	**Source**	DF	Seq SS	Adj SS	Adj MS	F	P
	Time (h)	5	614.2	614.2	122.84	4.19	0.036
	pH	2	198.3	198.3	99.16	3.38	0.086
	Dose (g/L)	2	414.4	414.4	207.18	7.07	0.017
	Residual Error	8	234.4	234.4	29.30		
	Total	17	1461.3				

process. This may be partly due to π-π interaction between the aromatic rings of anthracene and the aromatic structure in lignin, graphene oxide, and L-GO-PU.

The plot of qt against $t^{1/2}$ is multi-linear and deviating from the origin, represented in figure (7) indicating more than one process has affected the adsorption. Hence the first portion of the plot indicates the external mass transfer and the second portion is due to intra-particle or pore diffusion [16].

Table (6): Table of estimated parameters of kinetic modelsKinetic models

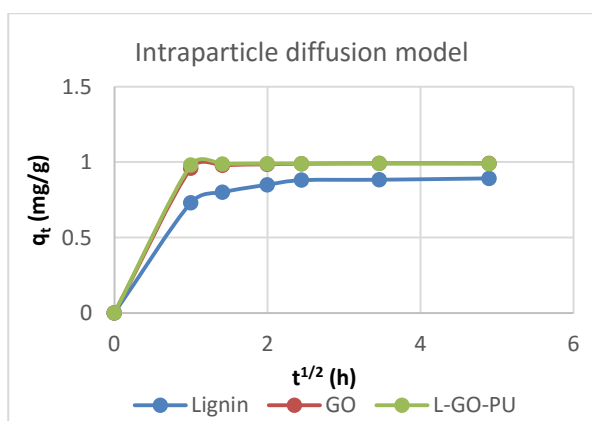|	Lignin	GO	L-GO-PU
Pseudo-first order			
k (1/h)	-0.59	-0.24	-0.16
R^2	0.84	0.80	0.78
Pseudo second order			
k_2(g/mg/h)	1.12	1.01	1.01
R^2	0.99	1	1
Intraparticle diffusion model			
k_i (mg/g/h$^{1/2}$)	0.14	0.14	0.14
R^2	0.49	0.37	0.36
C (mg/g)	0.42	0.54	0.55

Fig (7): intraparticle diffusion model of lignin, GO, L-GO-PU

Conclusions

Bio-based polyurethane was prepared using polymerization of extracted lignin from black liquor with castor oil, low percentage of graphene oxide and methylene diphenyl diisocyanate MDI. The results showed that lignin attain the ability of adsorbing anthracene by removing 89 %, 178 µg/L using contact time 24 hours and adsorbent dose 10 g/L. Furthermore, graphene oxide is a good adsorbent by removing 98.89 %, 197.78 µg/L by applying contact time 4 hours and adsorbent dose 10 mg/L. Notably, the polymerization of lignin forming polyurethane L-GO-PU increased the adsorption level to exceed lignin by adsorbing 98 %, 196 µg/L anthracene by applying contact time 1 hour and adsorbent dose 10 g/L. This may be due to the presence of castor oil and the decrease of the free polar groups that increased hydrophobicity of L-GO-PU.

The analysis according to Taguchi approach revealed the contribution of each factor studied. The contact time has a high contribution in adsorption process and ranked first in the experiments performed for lignin, GO, and L-GO-PU. Additionally, the adsorbent dose has a great effect but less than contact time and solution pH ranked the last.

The Taguchi approach in interpreting the acquired results suggest to indicate the optimum condition from signal to noise ratio results. The obtained data propose that optimum condition when using lignin is contact time 24 h, solution pH 7, and adsorbent dose 10 g/L. However, for GO and L-GO-PU, the optimum condition is contact time 6 h, solution pH 7, and adsorbent dose 5 g/L.

From the ANOVA study of acquired results: contact time have a significant effect on the adsorption of anthracene as the p-values were 0.017, 0.041 and 0.036 for lignin, GO, and L-GO-PU respectively. Beside contact time, adsorbent dose also possessed a significant effect on removing anthracene while p-values were 0.007 and 0.017 for lignin and L-GO-PU, otherwise GO has a less significance with p-value equal 0.055. Lastly, solution pH does not have a significant effect while p-values were 0.183, 0.224, and 0.086 for lignin, GO, and L-GO-PU.

The kinetic study of the adsorption process was performed to specify the reaction kinetic model of removing anthracene using lignin, GO and L-GO-PU. The results indicated that adsorption system follows a pseudo-second order kinetics which indicates a chemisorption reaction model. Also, by applying intra-particle kinetic model, the reaction rate was divided into two steps, the initial step possessed an increased reaction rate and the second step a decreased reaction rate which and could be described as follows, the first step is a mass transfer of anthracene onto the surface of the adsorbent.

4.References

1   D. Kai, M. J. Tan, P. L. Chee, Y. K. Chua, Y. L. Yap, and X. J. Loh,(2016) "Towards lignin-based functional materials in a sustainable world," Green Chem., vol. **18**, no. 5, pp. 1175–1200, , doi: 10.1039/c5gc02616d.

2   F. K. Ko, A. Goudarzi, L. T. Lin, Y. Li, and J. F. Kadla, (2016). Lignin-Based Composite Carbon Nanofibers. Elsevier Inc.,

3   C. Chen, M. Zhu, M. Li, Y. Fan, and R. C. Sun, (2016), "Epoxidation and etherification of alkaline lignin to prepare water-soluble derivatives and its performance in improvement of enzymatic hydrolysis efficiency," Biotechnol. Biofuels, vol. **9**, no. 1, pp. 1–15, doi: 10.1186/s13068-016-0499-9.

4   O. Oribayo, X. Feng, G. L. Rempel, and Q. Pan, (2017) "Synthesis of lignin-based polyurethane/graphene oxide foam and its

application as an absorbent for oil spill clean-ups and recovery," *Chem. Eng. J.*, vol. **323**, pp. 191–202, , doi: 10.1016/j.cej.2017.04.054.

5   Z. Shen, Y. Luo, Q. Wang, X. Wang, and R. Sun, (2014), "High-value utilization of lignin to synthesize ag nanoparticles with detection capacity For Hg2+," ACS Appl. Mater. Interfaces, vol. **6**, no. 18, pp. 16147–16155, doi: 10.1021/am504188k.

6   D. Feldman, M. Lacasse, and L. M. Beznaczuk, (1986), "Lignin-polymer systems and some applications," Prog. Polym. Sci., vol. **12**, no. 4, pp. 271–299, doi: 10.1016/0079-6700(86)90002-X.

7   L. Bruno, (2002)Chemical Modification, Properties, and Usage of Lignin, vol. **53**, no. 9. Boston, MA: Springer US,.

8   M. R. M. F. H. M. E. A. M. Gad, (2005) "Rheological Properties of OPC Pastes Made with Different Admixtures Sil.Ind. Volume **70** pp3-3." pp. 59–64,.

9   H. Wu, F. Chen, Q. Feng, and X. Yue, (2012) "Oxidation and sulfomethylation of alkali-extracted lignin from corn stalk," *BioResources*, vol. **7**, no. 3, pp. 2742–2751, , doi: 10.15376/biores.7.3.2742-2751.

10 W. Zhu, G. Westman, and H. Theliander, (2014) "Investigation and characterization of lignin precipitation in the lignoboost process," *J. Wood Chem. Technol.*, vol. **34**, no. 2, pp. 77–97, , doi: 10.1080/02773813.2013.838267.

11 O. Jankovský et al., (2016) "Synthesis procedure and type of graphite oxide strongly influence resulting graphene properties," Appl. Mater. Today, vol. **4**, pp. 45–53, , doi: 10.1016/j.apmt.2016.06.001.

12 S. L. Lee et al., (2019) "Sorption behavior of malachite green onto pristine lignin to evaluate the possibility as a dye adsorbent by lignin," Appl. Biol. Chem., vol. **62**, no. 1, , doi: 10.1186/s13765-019-0444-2.

13 F.-B. Liang, Y.-L. Song, C.-P. Huang, Y.-X. Li, and B.-H. Chen, (2013), "Synthesis of Novel Lignin-Based Ion-Exchange Resin and Its Utilization in Heavy Metals Removal," Ind. Eng. Chem. Res., vol. **52**, no. 3, pp. 1267–1274, Jan. doi: 10.1021/ie301863e.

14 F. Pendolino and N. Armata, (2017) "Synthesis, Characterization and Models of Graphene Oxide,", pp. 5–21.

15 M. Tanase-Opedal, E. Espinosa, A. Rodríguez, and G. Chinga-Carrasco, (2019), "Lignin: A biopolymer from forestry biomass for biocomposites and 3D printing," Materials (Basel)., vol. **12**, no. 18, pp. 1–15, doi: 10.3390/ma12183006.

16 J. Thilagan, S. Gopalakrishnan, and T. Kannadasan, (2013) "A study on Adsorption of Copper (II) Ions in Aqueous Solution by Chitosan - Cellulose Beads Cross Linked by Formaldehyde," vol. **2**, no. Ii, pp. 1043–1054,.